research articles Journal of proteome research

Different Residues in Channel Turret Determining the Selectivity of ADWX-1 Inhibitor Peptide between Kv1.1 and Kv1.3 Channels

Shi-Jin Yin,[†,#] Ling Jiang,[‡,#] Hong Yi,[#,†] Song Han,[†] Dai-Wen Yang,[§] Mai-Li Liu,[‡] Hui Liu,[†] Zhi-Jian Cao,[†] Ying-Liang Wu,[*,†] and Wen-Xin Li[*,†]

State Key Laboratory of Virology, College of Life Sciences, Wuhan University, Wuhan 430072, P. R. China, State Key Laboratory of Magnetic Resonance and Atomic and Molecular Physics, Wuhan Institute of Physics and Mathematics, Chinese Academy of Sciences, Wuhan, 430071, P. R. China, and Department of Biological Sciences, 14 Science Drive 4, National University of Singapore, Singapore 117543

Received July 3, 2008

The low selectivity of Kv1 peptide inhibitors for specific isoforms makes them poor candidates for the development of theraputics. Using combined approaches, we showed that the Kv1 turret is the critical determinant for ADWX-1 peptide inhibitor selectivity of Kv1.3 over Kv1.1. Mutation of Kv1.1 turret residues to match the sequence of Kv1.3 lead to increased inhibition of Kv1.1 activity. These studies may lead to improvements in peptide inhibitor drug development.

Keywords: Kv1.1 channel • Kv1.3 channel • channel turret • ADWX-1 peptide selectivity • structural basis

Introduction

Potassium channels are a diverse and ubiquitous family of membrane proteins present in both excitable and nonexcitable cells. The currents of many potassium channels can be inhibited by toxin peptides. Investigation of the interaction between inhibitory peptide toxins and potassium channels has provided a better understanding of the relationship between structure and function for potassium channels.[1−5] Recently, the structure of a mammalian Kv1.2-Kv2.1 potassium channel chimera showed that the architecture of the channel comprised six transmembrane regions (S1−S6) and a pore selectivity filter. While the structural information of the channel is critical to understanding its function, many fundamental questions of potassium channels still remain unanswered.[6,7] For example, the external vestibules vary among the different potassium channels. Thus, understanding how variation in the structure of the external vestibules translates into differential regulation of potassium channel function is key to understanding the functional diversity of potassium channels and to developing inhibitors selective for particular potassium channel isoforms, such as peptide inhibitors derived from certain animal venoms.

Since Kv1.3 potassium channel was demonstrated as the therapeutic target for T-cell mediated autoimmune diseases such as multiple sclerosis, type-1 diabetes, rheumatoid arthritis and psoriasis,[8−12] the development of specific peptide inhibitors has become an active field.[13] Unfortunately, the determinants of Kv1 channels for drug selectivity remains to be elucidated, and improvements in drug selectivity have been limited. For example, the ShK-L5 peptide, derived from the sea anemone toxin ShK, exhibited a 100-fold selectivity for Kv1.3 (IC_{50} = 69 pM) over Kv1.1 and *a* > 250-fold selectivity over all other tested channels.[9] A series of peptide analogues derived from the scorpion toxin OSK1 blocked Kv1.3 with improved selectivity through progressive deletions of N-terminal sequences.[14,15] At present, our group designed ADWX-1 peptide inhibited Kv1.3 channel current with IC_{50} value of 1.89 pM. This ADWX-1 lead also displayed the best selectivity on Kv1.3 over Kv1.1 and Kv1.2, for approximately 340-fold and $>10^5$-fold, respectively.[16] Although the specificity of these peptide inhibitors is much better than that of small chemical molecules,[13,17] selectivity improvement of peptide drug leads especially between Kv1.1 and Kv1.3 still remains an important challenge. This challenge stems from the lack of information about what sequences or structures of potassium channels determines the selective recognition by peptide toxins.

The two domains responsible for peptide specific recognition in the outer vestibule of potassium channels are the turret and the filter region (Figure 1). Using the ADWX-1 peptide as a probe, we determined the residues on the potassium channels that are responsible for the selectivity of ADWX-1 for Kv1.3 over Kv1.1. Through mutagenesis and computational experiments, we found that the Kv1 turret, but not the filter region, is responsible for the high selectivity of ADWX-1 peptide for Kv1.3 over Kv1.1. A mutant of the Kv1.1 channel (Kv1.1-AEHS/PSGN), in which four key residues of the Kv1.1 turret were replaced with the corresponding residues in Kv1.3 turret (Figure 1), had a similar sensitivity to ADWX-1 as the Kv1.3 channel. When computational models of the complex between ADWX-1 and the potassium channels were used, the turrets were found to associate with ADWX-1 peptide through both polar and nonpolar interactions. Additionally, while the turret arrangements were similar between the Kv1.1 and Kv1.3 channels, the Kv1.3

* To whom correspondence should be addressed. E-mail: Yingliang Wu (ylwu@whu.edu.cn) and Wenxin Li (liwxlab@whu.edu.cn).
† Wuhan University.
‡ Wuhan Institute of Physics and Mathematics.
# These authors contributed equally to the work.
§ National University of Singapore.

10.1021/pr800494a CCC: $40.75

Published on Web 10/21/2008

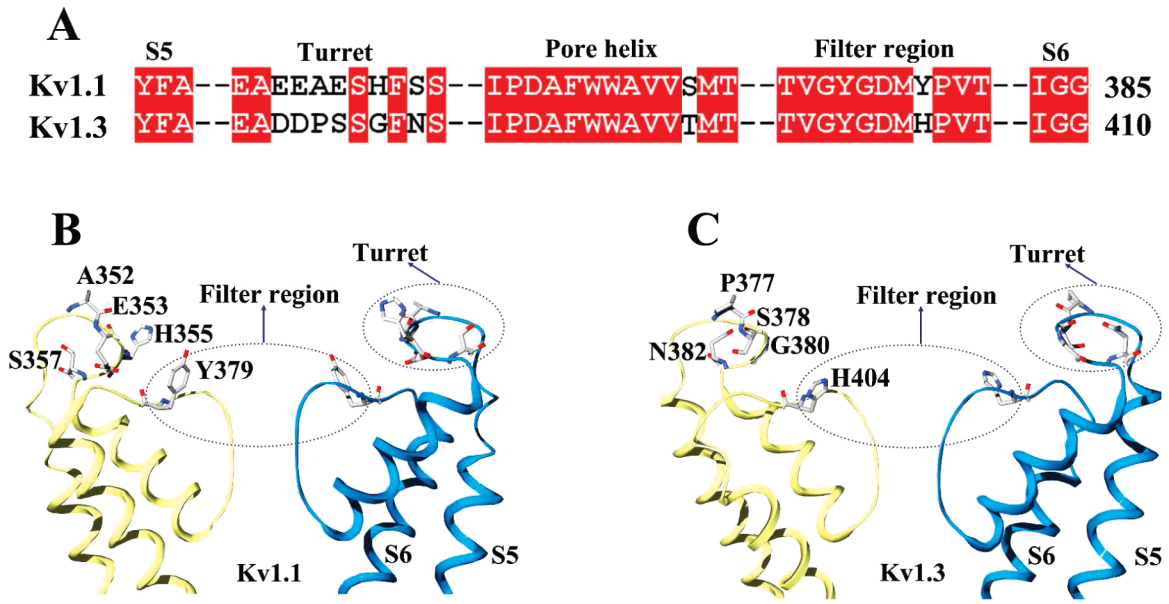

Figure 1. Sequence alignment and structural arrangement of the Kv1.1 and Kv1.3 channels. (A) The amino acid sequence alignment of the Kv1.1 and Kv1.3 channels. Red shaded letters show identical residues. (B and C) Models for the Kv1.1 (B) and Kv1.3 (C) channel. Circles in dashed line indicated the possible toxin-interacting surfaces.

turret bent more toward ADWX-1 peptide and made more intimate contacts with the peptide than did the turret of the Kv1.1 channel. Together, these findings revealed that contacts between the ADWX-1 peptide inhibitor and the potassium channel turret define the molecular basis for peptide selectivity, and will lead to better methods for the improvement of channel selectivity for future potassium channel inhibitors.

Materials and Methods

Peptides. ADWX-1 peptide was obtained as described previously.[16] Briefly, the coding sequence of the scorpion toxin BmKTX was used as the template for an overlap-extension PCR[18] to produce the cDNA of ADWX-1 and this was subcloned into pGEX-6P-1. Plasmid was then transformed into BL21 (DE3) Rosetta *Escherichia coli* cells for protein expression. Supernatant from the bacterial cell lysates was loaded onto a GST-bind column, the column was washed to remove unbound proteins, and the fusion protein was eluted in a buffer containing reduced glutathione. The purified fusion protein was desalted and enterokinase digestion was used to remove the GST tag from the ADWX-1 peptide. Protein samples were separated by HPLC on a C18 column and the ADWX-1 peptide was eluted as a major peak at 21−24% acetonitrile. The molecular mass of the purified ADWX-1 peptide was obtained by MALDI-TOF-MS (Voyager-DESTR, Applied Biosystems).

Nuclear Magnetic Resonance Spectroscopy and Structure Calculation. Nuclear magnetic resonance (NMR) measurements were carried out at 27 °C on a Varian INOVA 600 spectrometer. The NMR sample contained 1 mM ADWX-1, in 0.05% (w/v) NaN_3 and 25 mM phosphate buffer, pH 4.5 [90% H_2O and 10% D_2O (v/v)]. All of the chemical shifts were externally referenced to the methyl resonance of DSS (0 ppm). WATERGATE was employed for solvent suppression at the end of all the 2D experiments.[19] TOCSY with MLEV isotropic mixing times of 35 and 80 ms, and NOESY with mixing times of 100, 200, and 300 ms were collected in the phase-sensitive detection mode using a standard pulse sequence.[20] Data were processed using NMRPipe software[21] and analyzed with XEASY/Cara.[22]

Spatial structure calculations were performed using the program DYANA.[23] Upper distance restraints were determined from the NOESY spectrum with a mixing time of 100 ms, using the program CALIBA. Backbone dihedral angle restraints were derived from all the proton chemical shifts using TALOS.[24] The disulfide bonds (residues 7−27, 13−32, and 17−34) were uniquely determined from preliminary structure calculations and the corresponding restraints for d(Si, Sj), d(Ci, Sj), and d(Si, Cj) distances were introduced in subsequent calculation. Hydrogen bonds observed in at least 80% of preliminary structures were employed by their corresponding d(COi, HNj) and d(COi, Nj) distance restraints in subsequent calculation in accordance with the angle and distance criteria of hydrogen bonds. Amino acid side chain torsion angle restraints were obtained by analysis of local conformation and stereospecific assignments were double checked with the automated NOE assignment module in the CYANA2.1 program.[25]

In the final calculation, a family of 200 random structures were calculated by a DYANA simulated annealing protocol with 10 000-step. Twenty conformers with minimal target functions were selected and then subjected to a 2500-step energy minimization using the AMBER force field.[26] The quality of the resulting conformers was determined using PROCHECK-NMR.[27] The structure statistics for the 20 final structures are listed in Supplementary Table 1 (Supporting Information).

Electrophysiology. HEK293 cells were cultured in Dulbecco's modified Eagle's medium (DMEM) with 10% heat-inactivated fetal calf serum (Invitrogen Life Technologies, Carlesbad, CA) supplemented with ampicillin 100 units/mL and streptomycin 100 μg/mL. The cDNA of the mammalian Kv1.1 potassium channel (mKv1.1) and the mammalian Kv1.3 potassium channel (mKv1.3), in pBSTA and pSP64, respectively (kindly provided by Prof. Stephan Grissmer, University of Ulm, Ulm, Germany), were subcloned into the Xho I/BamH I sites of pIRES2-EGFP (Clontech). Correct insertion was confirmed by DNA sequencing. Plasmids containing mKv1.1and mKv1.3 were transfected into HEK293 cells using SofastTM Transfection Reagent (Sunma). Currents were recorded 1−3 days post-

transfection in cells expressing the enhanced green fluorescent protein (EGFP) marker.

Electrophysiological experiments were carried out at 22−25 °C using the patch-clamp whole-cell recording mode. Cells were bathed with mammalian Ringer's solution (5 mM KCl, 140 mM NaCl, 10 mM 4-(2-hydroxyethyl)-1-piperazineethanesulfonic acid (HEPES), 2 mM $CaCl_2$, 1 mM $MgCl_2$, 10 mM D-Glucose, pH 7.4, with NaOH). When ADWX-1 and the mutant toxin peptides were applied, 0.01% bovine serum albumin (BSA) was added to the Ringer's solution. A multichannel micro perfusion system MPS-2 (INBIO, Inc., Wuhan, China) was used to exchange the external recording bath solution. The pipet solution contained 140 mM KCl, 1 mM $MgCl_2$, 1 mM glycol-bis(2-aminoethylether)-*N,N,N′,N′*-tetraacetic acid (EGTA), 1 mM Na_2ATP, 5 mM HEPES, pH 7.4, with NaOH. Channel currents were elicited by depolarizing voltage steps of 200 ms from the holding potential −80 mV to +50 mV. Membrane currents were measured with an EPC 10 patch clamp amplifier (HEKA Elekt-ronik, Lambrecht, Germany) interfaced to a computer running acquisition and analysis software (Pulse).

Data analyses was performed with IgorPro (WaveMetrics, Lake Oswego, OR) and IC_{50} values were deduced by fitting a modified Hill equation to the data: $I_{toxin}/I_{control} = 1/1 + ([\text{toxin peptide}]/IC_{50})$, where I is the peak current to the normalized data points obtained with at least four different toxin peptide concentrations. Results are shown as mean ± SE, and n is the number of experiments, unless otherwise specified.

Atomic Coordinates and Molecular Docking. The mKv1.1 structure was modeled using KcsA (PDB code: 1BL8) as a template through the SWISSMODEL server.[28] The ZDOCK[29] program was used to obtain the possible candidates for a complex between ADWX-1 and Kv1.1. To improve the rigid performance of ZDOCK, several structures of ADWX-1 were used to predict the complexes between ADWX-1 and Kv1.1. Each docking experiment produced 2000 candidate complex structures. Possible hits were screened out by clustering the predictions with the results of the mutagenesis experiments, followed by a 500-step energy minimization and a 500 ps unrestrained molecular dynamics step performed on each plausible toxin peptide-channel complexes using the SANDER module in the AMBER 8 suit programs.[26]

Molecular Dynamic Simulations. The final model of the complex between ADWX-1 and Kv1.1 was sufficiently equilibrated to a 7 ns unrestrained molecular dynamic simulation to have enough flexibility for both the channel and toxin peptide.

All molecular dynamic (MD) simulations were carried out by using the Amber 8 program on a 66-CPU Dawning TC4000L cluster (Beijing, China). Temperature was set at 300 K and a cutoff distance of 12 Å was used for unbounded interactions. In this work, the generalized Born (GB) solvation model in macromolecular simulations[30,31] was used instead of explicit water during more sufficient MD simulation. The ff99 force field (Parm99)[32] was applied throughout the energy minimization and MD simulations. The detailed method was previously described.[33,34]

Results

The Filter Region of Kv1 Channels Does Not Determine ADWX-1 Sensitivity. Among Kv1.x channels, the two main domains that affect inhibitory peptide recognition are the filter region and the turret (Figure 1). The filter region, but not the turret, was found to be the critical determinant for the binding and inhibition of potassium channel activity by the BgK peptide from sea anemone venom and the maurotoxin peptide from scorpion venom.[35,36] Thus, we first sought to establish whether the filter region was also the critical determinant for ADWX-1 peptide binding and inhibition of the potassium channel.

Comparison of the amino acid sequence between Kv1.1 and Kv1.3 indicated that there is only a single residue change between these two isoforms (Figure 1). Both of these residues (Tyr379 in Kv1.1 and His404 in Kv1.3) were found to be critical for the binding of the sea anemone BgK peptide.[37] To determine if these residues were also critical for the binding of ADWX-1, we constructed a Kv1.1 mutant in which the Tyr379 was replaced by His, the corresponding residue in Kv1.3. Expression vectors encoding the wild-type Kv1.1 or Kv1.3 or the mutant Kv1.1-Y379H were used to transfect HEK293 cells, a human embryonic kidney cell line, and the potassium channel activity was measure in the presence of the ADWX-1 peptide to determine the sensitivity of each channel to the inhibitor. The effects of the ADWX-1 peptide on potassium channel currents elicited by 200-ms depolarizing pulses from a holding potential of −80 to 50 mV is shown in Figure 2A−C. As in our previous report,[16] there was a substantial difference ability of ADWX-1 to block the wild-type Kv1.1 and Kv1.3 channel activities. For the mutant Kv1.1-Y379H, only 60% of the current was inhibited by 100 pM of the ADWX-1 peptide (Figure 2B), whereas 10 pM of the ADWX-1 inhibited Kv1.3 by more than 60% (Figure 2C), indicating that there was a substantial difference in the sensitivity of these two channels to ADWX-1. The concentration−response curve for Kv1.1-Y379H in comparison with that of Kv1.1 and Kv1.3 is shown in Figure 2E. The IC_{50} value obtained for Kv1.1-Y379H was 65 pM, making the Kv1.1-Y379H channel about 10-fold more sensitive than the wild-type Kv1.1 channel ($IC_{50} = 0.66 \pm 0.25$ nM), and 34-fold less sensitive than the wild-type Kv1.3 channel ($IC_{50} = 1.90 \pm 0.53$ pM). Since the mutant Kv1.1-Y379H channel had a filter region that was identical to the filter region of Kv1.3 but a dramatic difference in ADWX-1 sensitivity (Figure 2B,C), then it was unlikely that the filter region was the critical determinant of ADWX-1 peptide selectivity.

To confirm our hypothesis that the filter region is unimportant for ADWX-1 potassium channel selectivity, we constructed a mutant Kv1.3 in which the His404 was replaced by Tyr, the corresponding residue in Kv1.1. As before, expression constructs for the wild-type and mutant channels were transfected into HEK293 cells and the potassium current was measured in the presence of the ADWX-1 inhibitor. The Kv1.3 and Kv1.3-H404Y channels have comparable binding affinity for the ADWX-1 (Figure 2C,D) and showed a similar concentration-dependent sensitivity to ADWX-1 (Figure 2F). For the Kv1.3-H404Y channel, the IC_{50} of ADWX-1 was 3.83 ± 0.69 pM, which makes Kv1.3-H404Y approximately 170-fold more sensitive to ADWX-1 than Kv1.1. These data further show that the filter region is not the critical determinant of ADWX-1 potassium channel selectivity and indicate that the potassium channel turret may be the candidate domain.

The Channel Turret of Kv1 Channels Determines ADWX-1 Selectivity. Comparison of the amino acid sequence of the turret domain between Kv1.1 and Kv1.3 (Figure 1) indicated that there are four resides that are different between the two channels. With the use of site-directed mutagenesis, the residues at these four positions in Kv1.1 were replaced by the corresponding amino acids in Kv1.3 individually or all four together. Two of the single residue substitution mutants, Kv1.1-

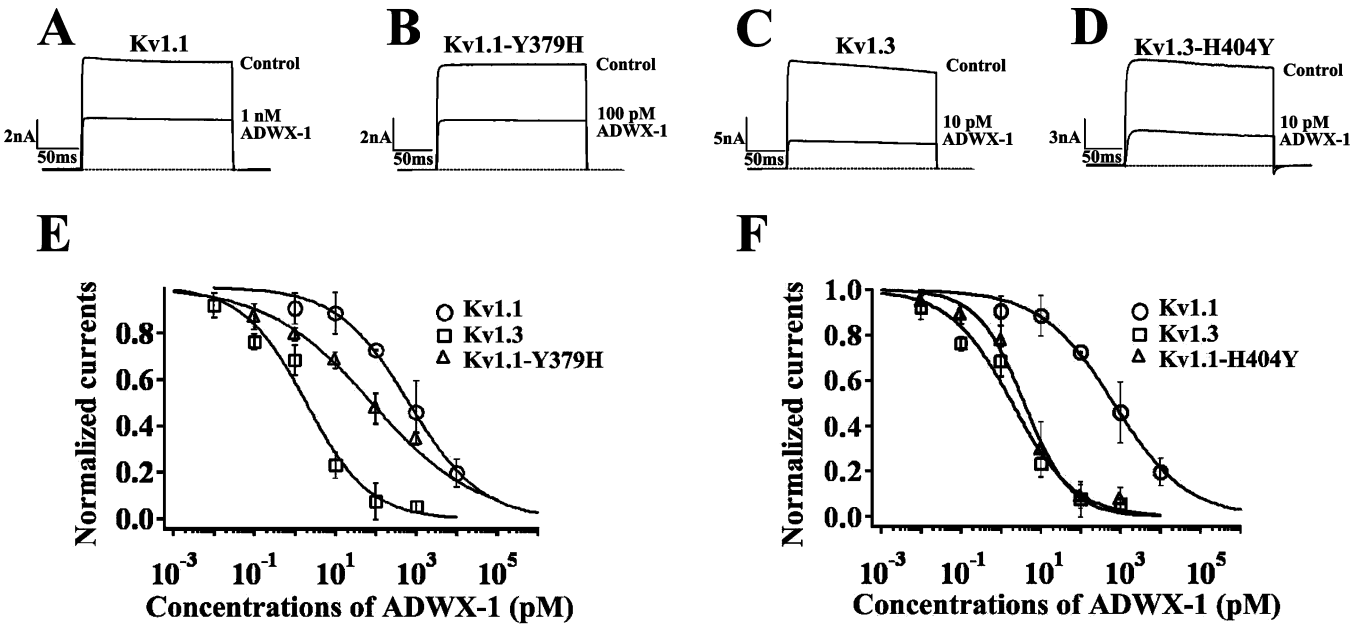

Figure 2. Affinity of ADWX-1 for filter region mutants of Kv1.1 and Kv1.3 channels. (A) Current traces in the absence (control) or presence of 1 nM ADWX-1 on Kv1.1 channels. (B) Current traces in the absence (control) or presence of 100 pM ADWX-1 on Kv1.1-Y379H mutant channels. (C) Current traces in the absence (control) or presence of 10 pM ADWX-1 on Kv1.3 channels. (D) Current traces in the absence (control) or presence of 10 pM ADWX-1 on Kv1.3-H404Y mutant channels. (E) Normalized current inhibition by various concentrations of ADWX-1 on Kv1.1, Kv1.1-Y379H, and Kv1.3 channels. (F) Normalized current inhibition by various concentrations of ADWX-1 on Kv1.1, Kv1.3-H404Y, and Kv1.3 channels. Data represent mean ± SE of at least three experiments.

E353S and Kv1.1-H355G, could not be expressed as functional channels. Since the structural difference between Gly and Ala is minimal, we constructed a Kv1.1-H355A mutant channel that was successfully expressed as a functional potassium channel. All together, four channel mutants (Kv1.1-A352P, Kv1.1-H355A, Kv1.1-S357N, and Kv1.1-AEHS/PSGN) were constructed, and upon expression in HEK293 cells, the mutants generated potassium currents with a comparable amplitude.

Of the three single residue substitution mutants, only the Kv1.1-A352P channel showed less sensitivity to ADWX-1 than wild-type Kv1.1 (Figure 3A). The Kv1.1-H355A mutant was slightly more sensitive to ADWX-1 than wild-type Kv1.1 (Figure 3B), and there was no difference in ADWX-1 sensitivity between the Kv1.1-S357N mutant and wild-type Kv1.1 (Figure 3C). The IC_{50} values of ADWX-1 for the Kv1.1-A352P, Kv1.1-H355A, and Kv1.1-S357N mutants were 1.38, 0.15, and 0.55 nM, respectively (Figure 3E). The low binding affinity of ADWX-1 to these mutants suggested that each single residue mutation alone was insufficient to recapitulate the high affinity ADWX-1 binding site found in Kv1.3. However, changing all four of these residues together should generate a Kv1.3-like ADWX-1 binding site in the Kv1.1 turret. To test this, the sensitivity of the Kv1.1-AEHS/PSGN mutant, in which the four different amino acids in Kv1.1 were simultaneously substituted to the corresponding residues in Kv1.3, was analyzed. Approximately 50% of the potassium current of Kv1.1-AEHS/PSGN channel was inhibited by 10 pM of the ADWX-1 peptide (Figure 3D), corresponding to an IC_{50} value of 3.94 pM (Figure 3F). This value was comparable to the ADWX-1 IC_{50} for Kv1.3 (IC_{50} = 1.90 ± 0.53 pM). Thus, by mutating the Kv1.1 turret sequence to match the sequence of the Kv1.3 turret, we were able to recapitulate the Kv1.3 sensitivity to the ADWX-1 inhibitor. These data indicate that the Kv1 turret domain is the critical determinant for ADWX-1 potassium channel selectivity.

NMR Solution Structure of ADWX-1. Although structures of the mammalian Kv1.2 and the Kv1.2-Kv2.1 chimera potassium channels have been determined,[38,39] the structures of the other potassium channels have yet to be determined and the structural determination of a potassium channel complexed with an inhibitory peptide remains a challenge. In a previous report, we used a combination of computational methods to reasonably show that the Kv1.2 turret bends away from the channel and does not influence difference in sensitivity between the Kv1.2 and Kv1.3 channels to the maurotoxin.[34] Using similar computational methods, we investigated the binding to the ADWX-1 peptide to the Kv1.1 channel.

First, we determined the structure of recombinant ADWX-1 by NMR. The structure of ADWX-1 in general shows the same overall topology as the wild-type BmKTX peptide,[40] which adopts a compact fold consisting of an α-helix and a strongly twisted antiparallel β-sheet (Figure 4). The α-helix of ADWX-1 peptide comprises residues Arg11 to Asp19, which is slightly longer than the BmKTX peptide α-helix, which consists of residues Leu14 to Ala20. However, the difference between two α-helix folding is trivial, because the extended Arg11−Cys13 segment in ADWX-1 is an atypical α-helix in the BmKTX peptide (Gly11−Cys13). The β-sheet is made of two antiparallel strands running from Lys26 to Ile28 and Lys31 to His33. Apart from the random structures in the N- and C-terminal segment (sequences 1−4 and 35−37), the root-mean-square deviations for Cα and backbone atoms are 1.12 and 1.24 Å, respectively, indicating there is no significant structure difference between ADWX-1 and BmKTX.

Conformational Differences between the Kv1.1 and Kv1.3 Turrets Determined by Computational Simulation. The pharmacological data demonstrated that the turret domains were the critical determinant of ADWX-1 selectivity between Kv1.1 and Kv1.3. To further characterize the role of the turret

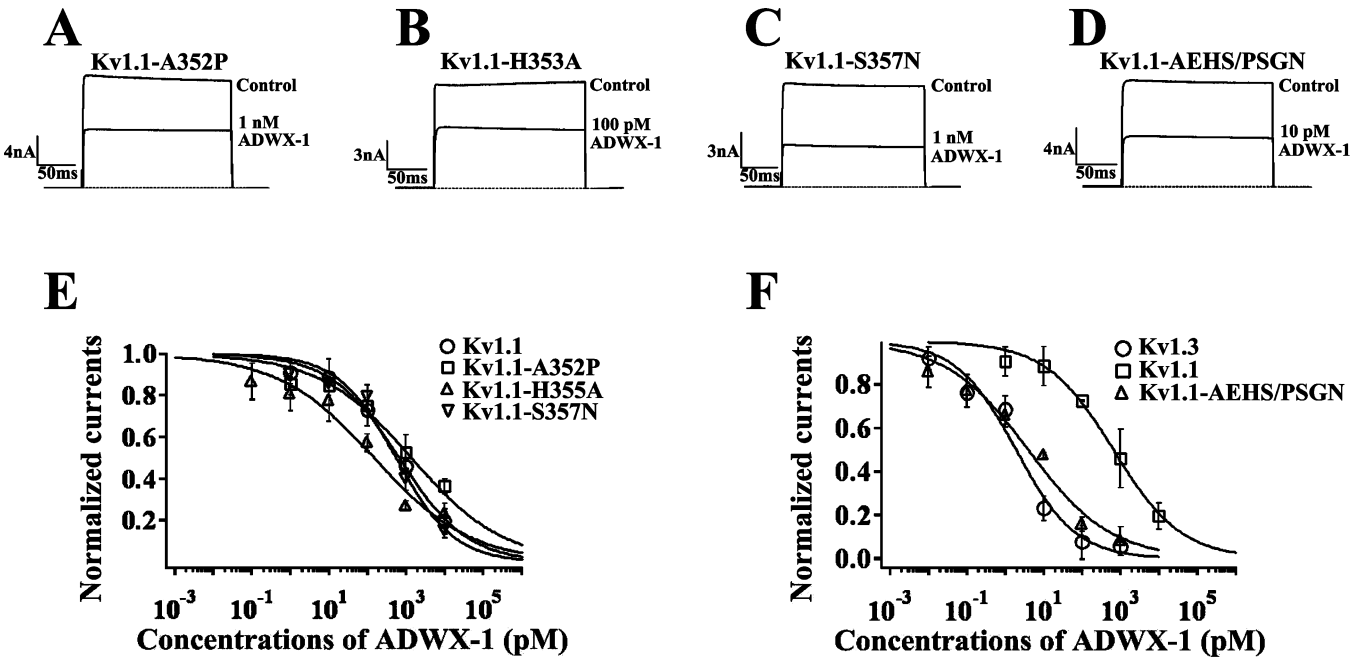

Figure 3. Affinity of ADWX-1 for turret region mutants of the Kv1.1 channel. (A) Current traces in the absence (control) or presence of 1 nM ADWX-1 on Kv.1.1-A352P channels. (B) Current traces in the absence (control) or presence of 100 pM ADWX-1 on Kv1.1-H355A channels. (C) Current traces in the absence (control) or presence of 1 nM ADWX-1 on Kv1.1-S357N channels. (D) Current traces in the absence (control) or presence of 10pM ADWX-1 on Kv1.1-AEHS/PSGN channels. (E) Normalized current inhibition by various concentrations of ADWX-1 on Kv1.1, Kv.1.1-A352P, Kv1.1-H355A and Kv1.1-S357N channels. (F) Normalized current inhibition by various concentrations of ADWX-1 on Kv1.1, Kv1.1-AEHS/PSGN and Kv1.3 channels. Data represent mean ± SE of at least three experiments.

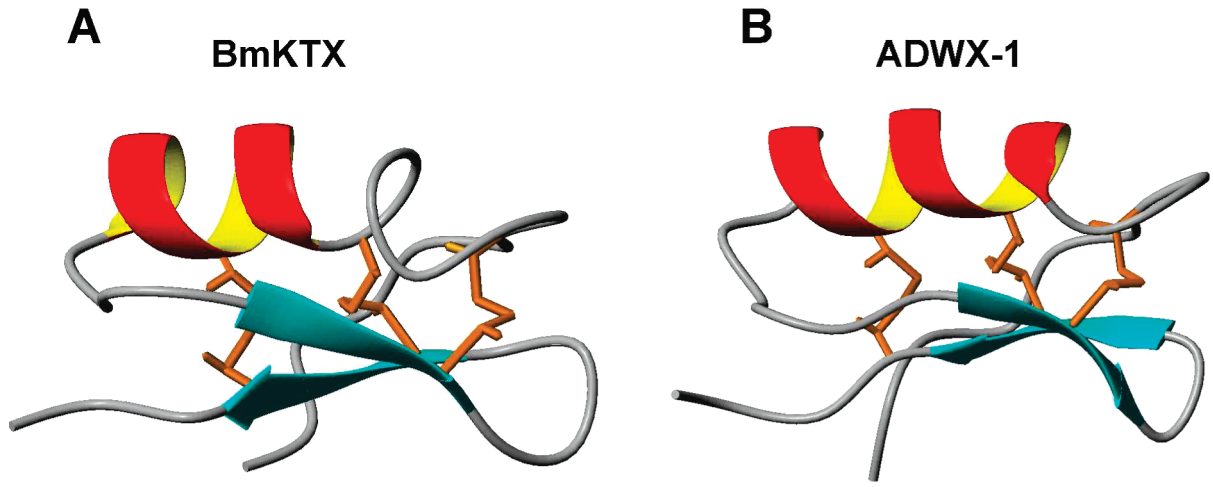

Figure 4. Comparison of the solution structures of BmKTX and ADWX-1. (A) Ribbon diagram of the BmKTX structure (PDB code: 1BKT). (B) Ribbon diagram of ADWX-1 structure (PDB code: 2K4U). The disulfide bridge patterns of both peptides are indicated.

sequence in this selectivity, we used the ADWX-1 structure to explore the conformational features of the Kv1.1 turret through combined computational methods.[33,34] First, the ADWX-1 structure was docked onto a Kv1.1 channel model using the rigid protein−protein program.[29] Second, we performed 500 ps molecular dynamic simulations to introduce protein flexibility for the docked results to screen for reasonable and stable candidates of the Kv1.1-ADWX-1 complex, and this process was assisted by the ADWX-1 functional information and interaction energy analysis.[41] Finally, an additional 7 ns unrestrained molecular dynamic simulations were carried out to sufficiently equilibrate the model of the Kv1.1-ADWX-1 complex prior to structure−function analysis of Kv1.1 channel.

As shown in Figure 5A,B, the overall structure of the complex between Kv1.1 and ADWX-1 is similar to that of Kv1.3 and ADWX-1, which was obtained by similar computational simulations and reported previously.[33,34] In both models, ADWX-1 adopts similar orientations above the outer vestibules of both the Kv1.1 and Kv1.3 channels, and there is minimal conformational difference in the filter regions between the Kv1.1 and the Kv1.3 models. However, the conformational features of the turret domain, induced by ADWX-1 peptide binding are different between of the Kv1.1 and Kv1.3 channels (Figure 5A,B). The conformational changes predominate in the A and C chains off the channel. The turret in the A chain is adjacent to the turn of the two antiparallel strands in the ADWX-1 peptide,

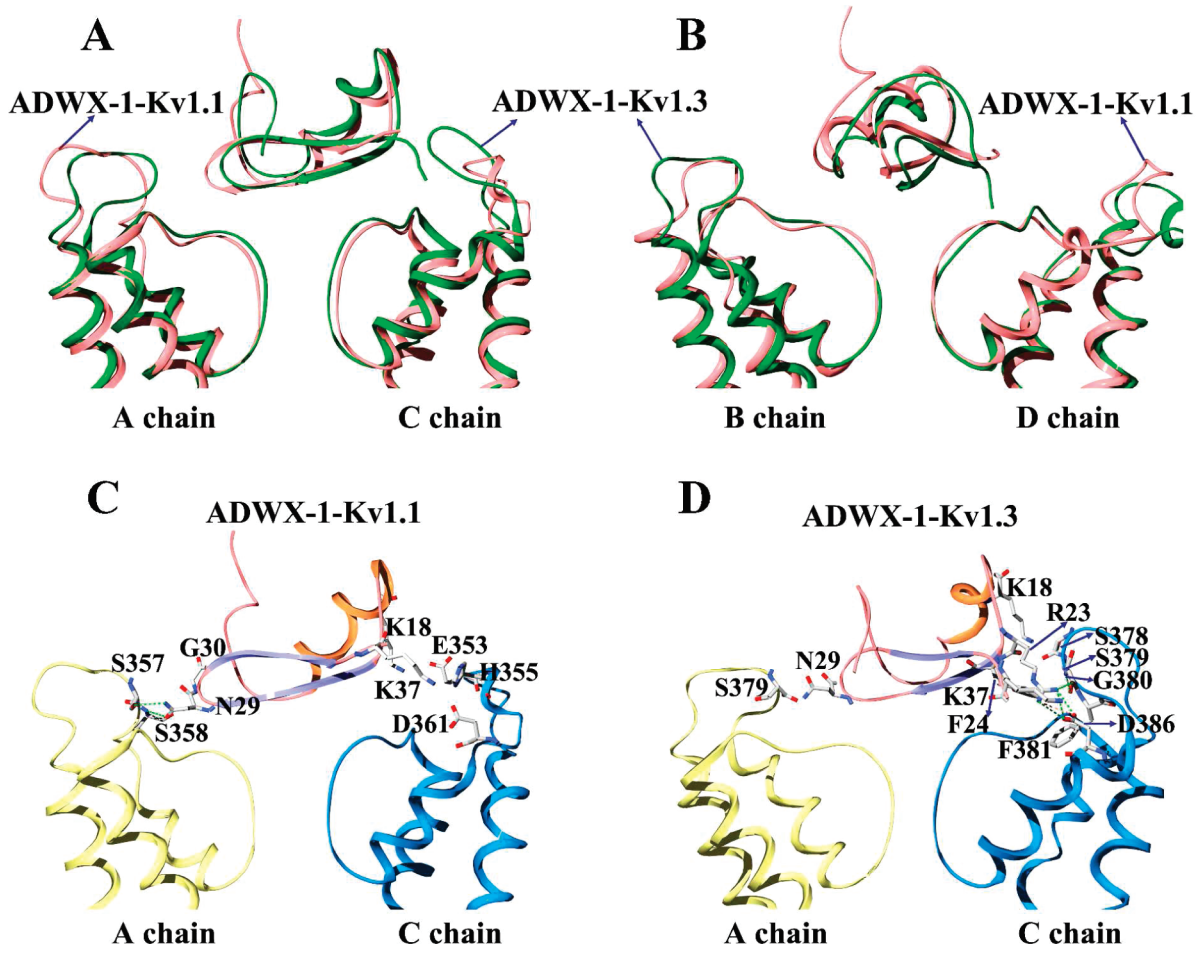

Figure 5. Structural comparison of ADWX-1-Kv1.1 and ADWX-1-Kv1.3 complexes. (A and B) Superposition of ADWX-1-Kv1.1 and ADWX-1-Kv1.3 complexes. For clarity, only the two opposite subunits of the Kv channels are shown in each column. (C) The Ser357, Glu353, His355, and Asp361 of Kv1.1 channel constitute the recognition surface of ADWX-1 within 4.0 Å. (D) The Ser379, Gly380, Phe381, and Asp386 of Kv1.3 channel constitute the recognition surface of ADWX-1 within 4.0 Å.

and the turret in the C chain closely approaches the turn between the α-helix and the second β-strand (Figure 5A). In contrast to the conformational change found in chains A and C, there are less structural differences between the B and D chains of Kv1.1 and Kv1.3. The turret of the D chain bends outward and is far from ADWX-1 peptide for both the Kv1.1 and Kv1.3 channels (Figure 5B). These data suggest that ADWX-1 binding can induce a conformational change of the four turrets of Kv1.1 and Kv1.3 to varying degrees, and the turrets of the A and C chains likely determine the selectivity of ADWX-1 between Kv1.1 and Kv1.3 channels.

To further characterize the influence of turrets on ADWX-1 selectivity, we investigated the residue-to-residue interactions at the channel-ADWX-1 peptide interfaces of the A and C chains. Within a contact distance of 4 Å, the Ser357 and Ser358 of the A chain of Kv1.1 can contact Asn29 and Gly30 of ADWX-1, leading to the formation of two hydrogen bonds (Figure 5C). A stronger interaction takes place between the turret of the Kv1.1 C chain and ADWX-1. The Glu353, His355, and Asp361 in the C chain likely interact with Lys18 and Lys37 of ADWX-1 through strong electrostatic interactions. The details of residue-to-residue interactions between the Kv1.3 turret and ADWX-1 are presented in Figure 5D. The Ser379 of the Kv1.3 A chain is adjacent to Asn29 of ADWX-1, indicating a little weaker interaction than that of the corresponding interaction between ADWX-1 and the Kv1.1 channel (Figure 5C). However, this interaction is likely compensated for by the much stronger interaction between the Kv1.3 C chain and ADWX-1, which is produced by polar and nonpolar interactions between residues Ser378, Ser379, Gly380, Phe381, and Asp386 of Kv1.3 and residues Lys18, Arg23, Phe24, and Lys37 of ADWX-1. These stronger interactions make the turret of the Kv1.3 C chain bend more toward ADWX-1 peptide than that of Kv1.1 (Figure 5A). The structural modeling agrees with the pharmacological data above, and together suggest that different conformation arrangements of the turrets and an overall weaker interaction between Kv1.1 and ADWX-1 likely contribute to the lower binding affinity of ADWX-1 peptide than that of Kv1.3.

Discussion

Molecular recognition and specific association of protein ligands and protein targets are central to most biological processes. Understanding the molecular basis of these interactions is critical for engineering novel protein−protein interactions and the rational design of peptide drugs. In particular, understanding how some ligands bind to subset of closely related receptors can greatly accelerate the design of drugs with the desired selectivity.

Currently, the biggest challenge for the development of drugs targeting T-cell mediated autoimmune diseases is the insufficient selectivity of Kv1.3 over Kv.1.1 by peptide inhibitors, such

as Shk-L5, OSK1, and ADWX-1.[9,14,16] Further, the molecular determinants of peptide inhibitor selectivity for Kv1 channel isoforms are largely unknown. The ADWX-1 peptide exhibits an approximately 340-fold specificity for Kv1.3 over Kv1.1, and served as a good molecular probe to investigate the molecular basis of ADWX-1 peptide selectivity. We used a combination of experimental and computational techniques to elucidate the residues of the Kv1 channel that determine the ADWX-1 selectivity.

Both the filter region and the turret of the potassium channel were investigated as candidate domains that could affect the specificity of peptide blockers (Figure 1) and the possibility of conformational changes induced by toxin peptide binding have been being increasingly studied.[33,42,43] Both the filter region and the turret contributed to the high selectivity of ADWX-1 for Kv1.3 over Kv1.1; however, the filter region had a negligible effect on the ADWX-1 selectivity, which was expected because the identical filter region between mutant and wild Kv1 channels led to less difference in ADWX-1 affinity (Figure 2). In contrast, the pharmacological data demonstrated that the turret played a definitive role in ADWX-1 selectivity, because there was a comparable affinity of ADWX-1 for the wild-type Kv1.3 channel and the Kv1.1 mutant that had a Kv1.3-like turret sequence (Kv1.1-AEHS/PSGN) (Figure 3D). Interestingly, the residues on Kv1 that determined the selectivity of ADWX-1 are different from the Kv1 residues that are targeted by the maurotoxin peptide, because turret residues of the Kv1.2 and Kv1.3 channels have little effect on the maurotoxin binding activity. In contrast, maurotoxin sensitivity appears to be determined by the filter region because substitution of His404 in the filter region of Kv1.3 channel with the corresponding Thr of the Shake channel caused an approximately 5500-fold increase in the maurotoxin binding affinity.[35] With the use of computational modeling of the ADWX-1 peptide complexed with either Kv1.1 and Kv1.3, the role of the turrets in ADWX-1 binding was well-characterized. The turrets of the A and C chains of Kv1.1 and Kv1.3 bent toward ADWX-1 and interacted with the peptide *via* both polar and nonpolar bonds (Figure 4A−D). Stronger contacts between ADWX-1 and Kv1.3 made the turret of the C chain bend more than that of Kv1.1, which could explain the about 340-fold difference in the sensitivity of ADWX-1 between Kv1.1 and Kv1.3. These data suggest that the conformation of the potassium channel turrets varies with different toxin peptides. For some peptide toxins the turrets are in the "open-state", in which the filter region plays a critical role of determining peptide potency and selectivity. This is the case for the binding of maurotoxin to the Kv1 channel. In other cases, the turrets are in the "half open-state" or "half closed-state", in which the turrets partially determine the potency and selectivity of the peptide toxin. This is the case for the binding of ADWX-1 to the Kv1 channels. Finally, the turrets could be in the "closed-state", in which four turrets and filter region simultaneously determine the potency and selectivity of a peptide toxin.

Potassium channels are the biggest family of ion channels. They are selectively recognized by hundreds of toxin peptides.[44] Using the selective ADWX-1 peptide as a molecular probe, we found that the flexible turrets with different residues and conformations were the critical determinants of the specificity of ADWX-1 for Kv1.3 over Kv1.1. The characterization of this interaction expands the knowledge of the structure−function relationship of potassium channels, and these detailed structures accelerated the development of selective potassium channel peptide blockers. Additionally, the identification of different conformations of the potassium channel outer vestibule will promote the use of toxin peptides as a starting point for the development of diagnostic and therapeutic agents specific for a given potassium channel isoform.

Acknowledgment. This work was supported by grants from the National Natural Sciences Foundation of China (Number: 30530140; 30570045; 30770519; 20605026; 20620140-104) and the Ministry of Education Foundation of China (Number: 106108).

Supporting Information Available: Supplementary Table 1, structural statistics for the group of the 20 lowest target function ADWX-1 structures. This material is available free of charge via the Internet at http://pubs.acs.org.

References

(1) Hidalgo, P.; MacKinnon, R. Revealing the architecture of a K+ channel pore through mutant cycles with a peptide inhibitor. *Science* **1995**, *268*, 307–310.
(2) MacKinnon, R.; Cohen, S. L.; Kuo, A.; Lee, A.; Chait, B. T. Structural conservation in prokaryotic and eukaryotic potassium channels. *Science* **1998**, *280*, 106–109.
(3) Ruta, V.; Jiang, Y.; Lee, A.; Chen, J.; MacKinnon, R. Functional analysis of an archaebacterial voltage-dependent K+ channel. *Nature* **2003**, *422*, 180–185.
(4) Lu, Z.; Klem, A. M.; Ramu, Y. Ion conduction pore is conserved among potassium channels. *Nature* **2001**, *413*, 809–813.
(5) Rodriguez de la Vega, R. C.; Merino, E.; Becerril, B.; Possani, L. D. Novel interactions between K+ channels and scorpion toxins. *Trends Pharmacol. Sci.* **2003**, *24*, 222–227.
(6) Ashcroft, F. M. From molecule to malady. *Nature* **2006**, *440*, 440–447.
(7) Yellen, G. The voltage-gated potassium channels and their relatives. *Nature* **2002**, *419*, 35–42.
(8) Beeton, C.; Wulff, H.; Standifer, N. E.; Azam, P.; Mullen, K. M.; Pennington, M. W.; Kolski-Andreaco, A.; Wei, E.; Grino, A.; Counts, D. R.; Wang, P. H.; LeeHealey, C. J.; rews, B. S.; Sankaranarayanan, A.; Homerick, D.; Roeck, W. W.; Tehranzadeh, J.; Stanhope, K. L.; Zimin, P.; Havel, P. J.; Griffey, S.; Knaus, H. G.; Nepom, G. T.; Gutman, G. A.; Calabresi, P. A.; Chandy, K. G. Kv1.3 channels are a therapeutic target for T cell-mediated autoimmune diseases. *Proc. Natl. Acad. Sci. U.S.A.* **2006**, *103*, 17414–17419.
(9) Beeton, C.; Pennington, M. W.; Wulff, H.; Singh, S.; Nugent, D.; Crossley, G.; Khaytin, I.; Calabresi, P. A.; Chen, C. Y.; Gutman, G. A.; Chandy, K. G. Targeting effector memory T cells with a selective peptide inhibitor of Kv1.3 channels for therapy of autoimmune diseases. *Mol. Pharmacol.* **2005**, *67*, 1369–1381.
(10) Wulff, H.; Calabresi, P. A.; Allie, R.; Yun, S.; Pennington, M.; Beeton, C.; Chandy, K. G. The voltage-gated Kv1.3 K(+) channel in effector memory T cells as new target for MS. *J. Clin. Invest.* **2003**, *111*, 1703–1713.
(11) Beeton, C.; Barbaria, J.; Giraud, P.; Devaux, J.; Benoliel, A. M.; Gola, M.; Sabatier, J. M.; Bernard, D.; Crest, M.; Beraud, E. Selective blocking of voltage-gated K+ channels improves experimental autoimmune encephalomyelitis and inhibits T cell activation. *J. Immunol.* **2001**, *166*, 936–944.
(12) Azam, P.; Sankaranarayanan, A.; Homerick, D.; Griffey, S.; Wulff, H. Targeting effector memory T cells with the small molecule Kv1.3 blocker PAP-1 suppresses allergic contact dermatitis. *J. Invest. Dermatol.* **2007**, *127*, 1419–1429.
(13) Wulff, H.; Pennington, M. Targeting effector memory T-cells with Kv1.3 blockers. *Curr. Opin. Drug Discovery Dev.* **2007**, *10*, 438–445.
(14) Mouhat, S.; Teodorescu, G.; Homerick, D.; Visan, V.; Wulff, H.; Wu, Y.; Grissmer, S.; Darbon, H.; De Waard, M.; Sabatier, J. M. Pharmacological profiling of Orthochirus scrobiculosus toxin 1 analogs with a trimmed N-terminal domain. *Mol. Pharmacol.* **2006**, *69*, 354–362.
(15) Mouhat, S.; Visan, V.; Ananthakrishnan, S.; Wulff, H.; reotti, N.; Grissmer, S.; Darbon, H.; De Waard, M.; Sabatier, J. M. K+ channel types targeted by synthetic OSK1, a toxin from Orthochirus scrobiculosus scorpion venom. *Biochem. J.* **2005**, *385*, 95–104.
(16) Han, S.; Yi, H.; Yin, S. J.; Chen, Z. Y.; Liu, H.; Cao, Z. J.; Wu, Y. L.; Li, W. X. Structural basis of a potent peptide inhibitor designed

for Kv1.3 channel, a therapeutic target of autoimmune disease. *J. Biol. Chem.* **2008**, *283*, 19058–19065.
(17) Panyi, G.; Possani, L. D.; Rodriguez de la Vega, R. C.; Gaspar, R.; Varga, Z. K+ channel blockers: novel tools to inhibit T cell activation leading to specific immunosuppression. *Curr. Pharm. Des.* **2006**, *12*, 2199–2220.
(18) Dai, L.; Wu, J. J.; Gu, Y. H.; Lan, Z. D.; Ling, M. H.; Chi, C. W. Genomic organization of three novel toxins from the scorpion Buthus martensi Karsch that are active on potassium channels. *Biochem. J.* **2000**, *346* (Pt 3), 805–809.
(19) Liu, M.; Mao, X.; Ye, C.; Huang, H.; Nicholson, J.; Lindon, J. Improved WATERGATE Pulse Sequences for Solvent Suppression in NMR Spectroscopy. *J. Magn. Reson.* **1998**, *132*, 125–129.
(20) Braun, S.; Kalinowski, H. O.; Berger, S. *150 and More Basic NMR Experiments.*, 2nd expanded ed.; Wiley-VCH: Weinheim, Germany, 1998; p 401−408.
(21) Delaglio, F.; Grzesiek, S.; Vuister, G. W.; Zhu, G.; Pfeifer, J.; Bax, A. NMRPipe: a multidimensional spectral processing system based on UNIX pipes. *J. Biomol. NMR* **1995**, *6*, 277–293.
(22) Bartels, C.; Xia, T.-H.; Billeter, M.; Guntert, P.; Wuthrich, K. The program XEASY for computer-supported NMR spectral analysis of biological macromolecules. *J. Biomol. NMR* **1995**, *6*, 1–10.
(23) Guntert, P.; Mumenthaler, C.; Wuthrich, K. Torsion angle dynamics for NMR structure calculation with the new program DYANA. *J. Mol. Biol.* **1997**, *273*, 283–298.
(24) Cornilescu, G.; Delaglio, F.; Bax, A. Protein backbone angle restraints from searching a database for chemical shift and sequence homology. *J. Biomol. NMR* **1999**, *13*, 289–302.
(25) Herrmann, T.; Guntert, P.; Wuthrich, K. Protein NMR structure determination with automated NOE assignment using the new software CANDID and the torsion angle dynamics algorithm DYANA. *J. Mol. Biol.* **2002**, *319*, 209–227.
(26) Case, D. A.; Darden, T.; Cheatham, T. E., III; Simmerling, C.; Wang, J.; Duke, R. E.; Luo, R.; Merz, K. M.; Wang, B.; Pearlman, D. A.; Crowley, M.; Brozell, S.; Tsui, V.; Gohlke, H.; Mongan, J.; Hornak, V.; Cui, G.; Beroza, P.; Schafmeister, C.; Caldwell, J. W.; Ross W. S.; Kollman, P. A. *Amber 8*; University of California: San Francisco, CA, 2004.
(27) Lovell, S.; Davis, I.; Arendall, W. r.; de Bakker, P.; Word, J.; Prisant, M.; Richardson, J.; Richardson, D. Structure validation by Calpha geometry: phi,psi and Cbeta deviation. *Proteins* **2003**, *50*, 437–450.
(28) Schwede, T.; Kopp, J.; Guex, N.; Peitsch, M. C. SWISS-MODEL: An automated protein homology-modeling server. *Nucleic Acids Res.* **2003**, *31*, 3381–3385.
(29) Chen, R.; Li, L.; Weng, Z. ZDOCK: an initial-stage protein-docking algorithm. *Proteins* **2003**, *52*, 80–87.
(30) Tsui, V.; Case, D. A. Molecular dynamics simulations of nucleic acids with a generalized Born solvation model. *J. Am. Chem. Soc.* **2000**, *122*, 2489–2498.
(31) Fan, H.; Mark, A. E.; Zhu, J.; Honig, B. Comparative study of generalized Born models: protein dynamics. *Proc. Natl. Acad. Sci. U.S.A.* **2005**, *102*, 6760–6764.
(32) Wang, J.; Cieplak, P.; Kollman, P. A. How well does a RESP(restrained electrostatic potential) model do in calculating the conformational energies of organic and biological molecules. *J. Comput. Chem.* **2000**, *21*, 1049–1074.
(33) Yi, H.; Cao, Z.; Yin, S.; Dai, C.; Wu, Y.; Li, W. Interaction simulation of hERG K(+) channel with its specific BeKm-1 peptide: insights into the selectivity of molecular recognition. *J. Proteome Res.* **2007**, *6*, 611–620.
(34) Yi, H.; Qiu, S.; Cao, Z.; Wu, Y.; Li, W. Molecular basis of inhibitory peptide maurotoxin recognizing Kv1.2 channel explored by ZDOCK and molecular dynamic simulations. *Proteins* **2008**, *70*, 844–854.
(35) Visan, V.; Fajloun, Z.; Sabatier, J. M.; Grissmer, S. Mapping of maurotoxin binding sites on hKv1.2, hKv1.3, and hIKCa1 channels. *Mol. Pharmacol.* **2004**, *66*, 1103–1112.
(36) Gilquin, B.; Braud, S.; Eriksson, M. A.; Roux, B.; Bailey, T. D.; Priest, B. T.; Garcia, M. L.; Menez, A.; Gasparini, S. A variable residue in the pore of Kv1 channels is critical for the high affinity of blockers from sea anemones and scorpions. *J. Biol. Chem.* **2005**, *280*, 27093–27102.
(37) Gilquin, B.; Racape, J.; Wrisch, A.; Visan, V.; Lecoq, A.; Grissmer, S.; Menez, A.; Gasparini, S. Structure of the BgK-Kv1.1 complex based on distance restraints identified by double mutant cycles. Molecular basis for convergent evolution of Kv1 channel blockers. *J. Biol. Chem.* **2002**, *277*, 37406–37413.
(38) Long, S. B.; Tao, X.; Campbell, E. B.; MacKinnon, R. Atomic structure of a voltage-dependent K+ channel in a lipid membrane-like environment. *Nature* **2007**, *450*, 376–382.
(39) Long, S. B.; Campbell, E. B.; Mackinnon, R. Crystal structure of a mammalian voltage-dependent Shaker family K+ channel. *Science* **2005**, *309*, 897–903.
(40) Renisio, J. G.; Romi-Lebrun, R.; Blanc, E.; Bornet, O.; Nakajima, T.; Darbon, H. Solution structure of BmKTX, a K+ blocker toxin from the Chinese scorpion Buthus Martensi. *Proteins* **2000**, *38*, 70–78.
(41) Case, D. A.; Cheatham, T. E., 3rd; Darden, T.; Gohlke, H.; Luo, R.; Merz, K. M., Jr.; Onufriev, A.; Simmerling, C.; Wang, B.; Woods, R. J. The Amber biomolecular simulation programs. *J. Comput. Chem.* **2005**, *26*, 1668–1688.
(42) Lange, A.; Giller, K.; Hornig, S.; Martin-Eauclaire, M. F.; Pongs, O.; Becker, S.; Baldus, M. Toxin-induced conformational changes in a potassium channel revealed by solid-state NMR. *Nature* **2006**, *440*, 959–962.
(43) Zachariae, U.; Schneider, R.; Velisetty, P.; Lange, A.; Seeliger, D.; Wacker, S. J.; Karimi-Nejad, Y.; Vriend, G.; Becker, S.; Pongs, O.; Baldus, M.; de Groot, B. L. The molecular mechanism of toxin-induced conformational changes in a potassium channel: relation to C-type inactivation. *Structure* **2008**, *16*, 747–754.
(44) Rodriguez de la Vega, R. C.; Possani, L. D. Current views on scorpion toxins specific for K+-channels. *Toxicon* **2004**, *43*, 865–875.

PR800494A